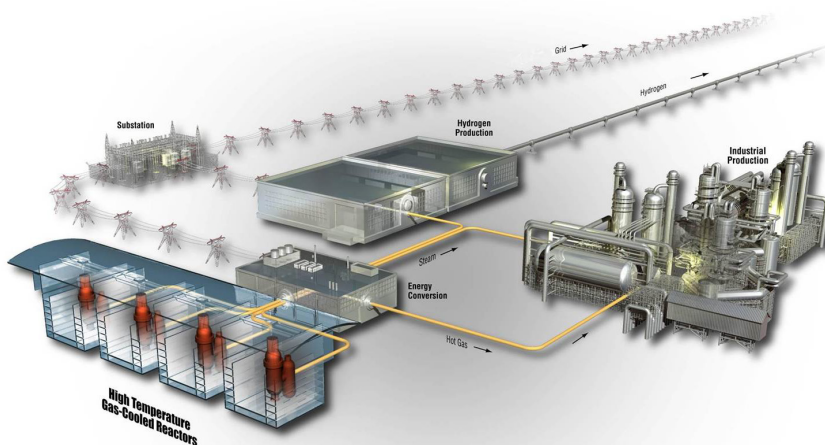


Preliminary Investigation of the Effect of AGC-2 Irradiation on the Strength of Different Grades of Nuclear Graphites

Mark Carroll

July 2015

The INL is a
U.S. Department of Energy
National Laboratory
operated by
Battelle Energy Alliance



DISCLAIMER

This information was prepared as an account of work sponsored by an agency of the U.S. Government. Neither the U.S. Government nor any agency thereof, nor any of their employees, makes any warranty, expressed or implied, or assumes any legal liability or responsibility for the accuracy, completeness, or usefulness, of any information, apparatus, product, or process disclosed, or represents that its use would not infringe privately owned rights. References herein to any specific commercial product, process, or service by trade name, trade mark, manufacturer, or otherwise, does not necessarily constitute or imply its endorsement, recommendation, or favoring by the U.S. Government or any agency thereof. The views and opinions of authors expressed herein do not necessarily state or reflect those of the U.S. Government or any agency thereof.

Preliminary Investigation of the Effect of AGC-2 Irradiation on the Strength of Different Grades of Nuclear Graphites

Mark Carroll

July 2015

**Idaho National Laboratory
INL ART TDO Program
Idaho Falls, Idaho 83415**

<http://www.inl.gov>

**Prepared for the
U.S. Department of Energy
Office of Nuclear Energy
Under DOE Idaho Operations Office
Contract DE-AC07-05ID14517**

INL Advanced Reactor Technologies Program

**Preliminary Investigation of the Effect of AGC-2
Irradiation on the Strength of Different Grades of
Nuclear Graphites**

INL/EXT-15-36044
Revision 0

July 2015

Author:



Mark C. Carroll
INL Senior Staff Scientist

7-27-2015

Date

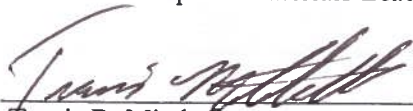
Approved by:



William E. Windes
INL ART Graphite Materials Lead

7/27/2015

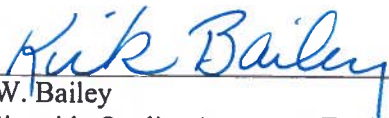
Date



Travis R. Mitchell
INL ART Program Manager

7/27/2015

Date



Kirk W. Bailey
INL Sitewide Quality Assurance Engineer

7-27-2015

Date

ABSTRACT

This report details the initial comparison of mechanical strength properties between the cylindrical nuclear-grade graphite specimens irradiated in the second Advanced Graphite Creep (AGC-2) experiment with the established baseline, or unirradiated, mechanical properties compiled in the Baseline Graphite Characterization program. The overall comparative analysis describes the development of an appropriate test protocol for irradiated specimens and execution of mechanical tests on the AGC-2 sample population, and further discusses the data in terms of developing an accurate irradiated property distribution in the limited amount of irradiated data by leveraging the considerably larger property datasets being captured in the Baseline Graphite Characterization program. The comparison between irradiated AGC-2 specimens and unirradiated “sister” specimens of the same geometry machined from the same sections of the original graphite billets demonstrates the expected increase in mechanical strength following irradiation. The comparison between the non-standard three-point bend test developed for determining the flexural strength of the AGC specimens is further compared to four-point bend testing on standard specimens of the geometry and test procedure prescribed by ASTM International. Integrating information on the inherent variability in nuclear-grade graphite with more complete datasets allows the establishment of a comprehensive body of data that can provide both a direct and indirect indication of the full irradiated property distributions that can be expected of irradiated nuclear-grade graphite while in service in a VHTR system. While the most critical data will remain the actual irradiated property measurements, expansion of this data into accurate distributions based on the inherent variability in graphite properties is a crucial step in qualifying graphite for nuclear use as a structural material in a VHTR environment.

CONTENTS

ABSTRACT.....	vii
ACRONYMS.....	xiii
1. INTRODUCTION.....	1
2. EXPERIMENTAL PROCEDURES.....	2
2.1 Test Selection.....	2
2.2 Three-Point Flexural Testing	3
2.3 Experimental Results	8
3. DISCUSSION.....	17
4. FUTURE WORK	24
5. REFERENCE	25

FIGURES

Figure 1. Tensile testing on cylindrical graphite specimens using a standard tensile fixture can be carried out by gluing specimens to threaded connectors that are fastened to shoulder sections with an appropriate ring groove. The procedure, described in ASTM C781, may not be the most robust approach to collecting qualified data from limited specimens.....	2
Figure 2. Graphic example of a tensile specimen machined from graphite per the geometry of ASTM C749.	3
Figure 3. Finite element modeling of a three-point bend test on a cylinder with a 2-to-1 height to diameter ratio shows the desired buildup of tensile stress along the lateral tensor σ_{33} at the lower section of the specimen directly between the load rollers. Only half of the symmetrical configuration is shown.	4
Figure 4. The common fracture paths in a sub-sized flexural specimen under three-point loading. The green arrow shows the desired fracture path due to flexural stress, while the red arrow show two directions of failure that initiate at the support roller contact point.	5
Figure 5. Examples of the fractures that initiate at the load roller contact point, as observed during the scoping study to determine the most appropriate configuration to facilitate reproducible failure in flexure. The left example shows compressive failure due to the support roller being too close to the outer edge; the right example shows compressive failure at the roller resulting from an inadequate margin between tensile loading at the lower midpoint and compressive stress at the roller contact point.	5
Figure 6. The simulated stress field around a roller-specimen contact point demonstrates the interaction of the stress with the free surface at the end of the specimen. The inability to accommodate this stress with surrounding graphite can lead to end failures of the specimen.	6

Figure 7. The reduction in stress due to larger roller diameters is shown by the magnitude of the stresses in the filed surrounding the contact with a 4.5 mm roller (left) and a 9 mm roller (right).	7
Figure 8. The final setup as run for the scoping study (left) resulted in fracture at the maximum tensile stress due to flexural loading, resulting in fracture at the midpoint of the specimen as shown schematically (right).	8
Figure 9. The load frame in the Carbon Characterization Laboratory	9
Figure 10. A coordinated effort between a frame operator (right), a technician who handles and loads the irradiated specimens (center), and radiological controls monitoring (left) ensure an effective test protocol for AGC specimens.....	9
Figure 11. A representative load-deflection curve for the initial mechanical testing on AGC-2 specimens shows the increase in both strength and modulus following irradiation as compared to the unirradiated sister specimen. This particular sample was NBG-17.	10
Figure 12. The fracture in the stronger fine-grained graphite grades indicated that the irradiation effects reduced the effectiveness of the approved fixture configuration with regard to preventing fracture initiation at the support rollers.	11
Figure 13. An increase in roller size from 9 mm to 12 mm provides a further reduction in compressive stress at the roller contact point, reducing the likelihood for support roller fracture initiation.	11
Figure 14. The modified flexure assembly utilizes a shortened upper (load) shaft to minimize lateral deflection, a rigid load contact radius rather than a roller, and larger 12 mm support rollers. The modified configuration was effective at reducing roller contact failure.....	12
Figure 15. Weibull probability density functions for flexural strengths of the unirradiated sister specimens show the comparative strength levels between candidate graphite grades.	14
Figure 16. The irradiated AGC-2 strength distributions show a similar trend in relative strengths between grades, along with the expected increase in values following the AGC-2 exposure.....	15
Figure 17. The individual shifts in strength for each of the candidate grades between the unirradiated sister specimens and the specimens irradiated in AGC-2.....	16
Figure 18. Quantification of the strength increases based on the Weibull scale factors shows the measurable increase in representative flexural strengths following irradiation.....	17
Figure 19. Comparisons between both the irradiated and unirradiated three-point test results and the standard four-point bend results from the Baseline program indicate significant differences in measured values. Integration of the trends seen in datasets must consider not only external effects such as temperature and dose but also effects due to the specific test approach.....	19
Figure 20. A comparison of flexural strength results for NBG-18 indicates considerably less variability (as evidenced by the higher Weibull shape parameter) for the comprehensive Baseline data set. The variability in AGC-2 strength data conservatively exhibits higher variability.....	20
Figure 21. The comparison of flexural strength results from PCEA indicates that the appropriate level of inherent variability in the graphite grade is not reflected in the AGC-2 strength	

distribution. The overall probably strength distribution for irradiated properties must consider this higher level of variability.	21
Figure 22. IG-110 exhibits a level of variability in measured flexural strengths that is comparable between the different test and conditions. The AGC-2 strength results show slightly less variability than should be expected based on the larger Baseline data level of inherent property variability.	22
Figure 23. Preliminary analysis suggests that a measurable peak in the flux profile at the core midpoint resulted in higher dose and temperature exposure to specimens near the center of the test train. Examples of grouping the results by “high” and “low” dose and temperature values based solely on position in the core indicate that a difference in final properties does exist.	23

TABLES

Table 1. The specimens taken from the un-stressed AGC-2 inventory for mechanical testing, along with a selection of sister specimens to provide comparative strength values.	13
Table 2. The listed Weibull scalar values for comparison between the tests. The comparison between unirradiated sister specimens in three-point bending differs significantly from unirradiated specimen testing on Baseline specimens in four-point bending.	17

ACRONYMS

AGC	Advanced Graphite Creep experiment
ART	Advanced Reactor Technologies
ASME	American Society of Mechanical Engineers
CCL	Carbon Characterization Laboratory
dpa	Displacements per atom
ECAR	Engineering Calculation and Analysis Report
INL	Idaho National Laboratory
ORNL	Oak Ridge National Laboratory
RBA	Radiological Buffer Area
VHTR	Very High Temperature Reactor

Preliminary Investigation of the Effect of AGC-2 Irradiation on the Strength of Different Grades of Nuclear Graphites

1. INTRODUCTION

This report details the initial comparison of mechanical strength properties between the cylindrical nuclear-grade graphite specimens irradiated in the second Advanced Graphite Creep (AGC)-2 experiment (PLN-3267, “AGC-2 Characterization Plan”¹) with the established baseline, or unirradiated, mechanical properties compiled in the Baseline Graphite Characterization program (PLN-3467, “Baseline Graphite Characterization Plan: Electromechanical Testing”²). Very high temperature reactor (VHTR) research on nuclear-grade graphite as a structural core material, being carried out as a portion of the overarching Advanced Reactor Technologies (ART) program, is a joint effort between the Idaho National Laboratory (INL) and Oak Ridge National Laboratory (ORNL). As part of the division of effort and responsibilities, ORNL received the irradiated AGC-1 specimens in 2014 for mechanical testing and INL carried out testing on a cross-section of AGC-2 specimens, nominally targeted for 3-4 dpa at 600°C, in FY2015. The comparative analysis will describe the development of an appropriate test protocol for irradiated specimens, the execution of the mechanical tests on the AGC-2 sample population, and will further discuss the data in terms of developing an accurate irradiated property distribution in the limited amount of irradiated data by leveraging the considerably larger property datasets being captured in the Baseline Graphite Characterization program. Integrating information on the inherent variability in nuclear-grade graphite with more complete datasets is one of the goals of the ART Graphite Materials program. Between “sister” specimens, or specimens with the same geometry machined from the same sub-block of graphite from which the irradiated AGC specimens were extracted, and the comprehensive Baseline datasets, a thorough body of data is being developed that provides both a direct and indirect indication of the full irradiated property distributions that can be expected of irradiated nuclear-grade graphite while in service in a VHTR system. While the most critical data for VHTR use will remain the actual irradiated property measurements, expansion of this data into accurate distributions based on the inherent variability in graphite properties will be a crucial step in qualifying graphite for nuclear use as a structural material in a VHTR environment.

The development of an American Society of Mechanical Engineers (ASME) code that sets the parameters for use of graphite as a structural material in Generation IV nuclear reactors will depend significantly on appropriate strength property information that is drawn from the AGC experiments. In order to support the compilation of a detailed set of physical and mechanical properties on nuclear graphite grades, the standard strength tests being employed in the Baseline Graphite Characterization program (tensile, flexural, and compressive) are all carried out on specimens that are machined to the prescribed dimensions of the standards published by the ASTM International for those individual tests. ASTM C749,³ ASTM C651,⁴ and ASTM C695⁵ provide the approved and published procedure for tensile, flexural, and compressive testing, respectively. The ASME committee, having not prescribed a specific test from which to draw strength property information, provided an opportunity for the graphite research leads at INL and ORNL to decide on the most effective means to test the irradiated specimens from the AGC experiments in order to support ASME-based evaluations.

2. EXPERIMENTAL PROCEDURES

2.1 Test Selection

As tensile strength is a limiting strength parameter in graphite, tensile testing might seem like the obvious choice for irradiated AGC specimen evaluations. Despite the simple specimen size and shape limitations imposed by the AGC load configuration, a procedure for tensile testing graphite in the cylindrical geometry being used for AGC creep specimens (Figure 1) is described in ASTM C781,⁶ in which cylindrical specimens are glued at either end to threaded connectors that attach to a shoulder section with a ring groove that resembles the monolithic tensile specimens described in ASTM C749 (Figure 2). This test approach was used in a preliminary evaluation of strength of AGC-1 sister specimens, as reported in ORNL/TM-2009/025 “AGC-1 Sister Specimen Testing Data Report.”⁷ As the report describes, considerable difficulty was encountered in producing valid test data due to the large fraction of failures that occurred near the glue joint. Per the applicable test standard and test-specific annex in ASTM C781, the location of fracture in the specimens with failure near the joint render the associated data as non-reportable. With the limited number of specimens available from the AGC experiments from which to draw strength data, having invalidated tests is of considerable concern. Additionally, aside from the inherent complexity in gluing irradiated specimens in a manner that ensures a high probability of appropriate fracture character, the containment issues in bagging a mechanical test specimen in a load train were determined to be unfavorable due to the additional radiological waste that would be produced when gluing additional material to the actual specimens. Taking these concerns into consideration, an analysis of mechanical strength via flexural or compressive tests would have a distinct benefit in that they rest independently between the load and support fixtures, without the need for pre-test gluing or additional handling, and can be individually bagged for the test as a primary means of radiological containment.



Figure 1. Tensile testing on cylindrical graphite specimens using a standard tensile fixture can be carried out by gluing specimens to threaded connectors that are fastened to shoulder sections with an appropriate ring groove. The procedure, described in ASTM C781, may not be the most robust approach to collecting qualified data from limited specimens.

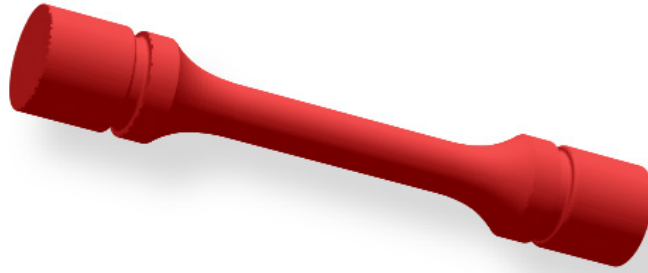


Figure 2. Graphic example of a tensile specimen machined from graphite per the geometry of ASTM C749.

A scoping study to detail the viability of flexural or compression testing on the AGC specimens was carried out in 2014. The AGC creep specimens, with their cylindrical geometry and 12.7 to 6.35 mm height to diameter ratio, are ideally suited to compression testing as they perfectly match the shape and ratio required by ASTM C695. As testing of bagged specimens demonstrated, however, the consistently high displacement of one of the two halves of the compressive specimen at the contact surface between the specimen and the fixture platens during fracture resulted in significant tears to the polyethylene bags being used as containment barriers, regardless of the thickness. Another concern is that even successful compression test results would be of somewhat limited value in that tensile strength is the more limiting property in graphite, and compressive tests do not provide data that can be related to the tensile strength.

2.2 Three-Point Flexural Testing

Flexural testing, in which the failure mode in an appropriate test is a tensile failure at the outer fibers of the material between the support rollers, does provide tensile strength information along with the ideal and relatively straightforward containment scenario. The AGC-based geometry, however, is the least favorable of the three types of mechanical strength tests with regard to meeting the prescriptive requirements of the governing ASTM standard. The small length to diameter ratio precludes the use of a four-point bend test, and the recently approved three-point bend test for evaluating the flexural strength of graphite (ASTM D7972⁸) recommends a length to diameter ratio of at least 6. The potential for an effective three-point flexure test with the limited geometry depends upon a number of factors, with the ideal result being a tensile stress at the center of the specimen in bending that facilitates fracture at the mid-point opposite the load roller. Figure 3 demonstrates the stress profile in a half-geometry finite element simulation of a three-point test with the AGC creep specimen configuration, in which the largest concentration of stress along the tensile σ_{33} tensor is shown at the mid-point of the specimen. Factors that might preclude this ideal fracture character would include crack initiation at the roller contact point or failure characterized by a separation of the outside of the cylinder at the roller contact point (Figure 4 and Figure 5). For the latter condition, too wide a support roller spacing will result in a limited amount of volume to constrain the compressive stress field around the support roller. The proximity to the free surface at the end of the specimen can thereby provide a failure path from the roller surface to the unconstrained outer edge of the specimen. Figure 6 demonstrates the interaction between the compressive stress component at roller surface and the free surface at the specimen end. Although no detailed information was analyzed that shows the exact stress level that would allow a fracture to propagate between the roller and the free surface, testing to failure and post-test observation quickly indicate whether this mode is occurring. Adjustments to move the support roller closer together and the resulting fracture observed in subsequent tests indicate whether the reduced spacing is adequate to prevent this mode of failure. The compromise in moving the roller spacing closer together, however, is the increase in compressive stress at the contact point of the roller relative to the tensile stresses building at the midpoint

of the specimen due to the induced flexure stress. For three-point bend testing of a right circular cylinder, the presumptive relationship for the calculation of flexure stress is:

$$\sigma_f = PL/\pi r^3$$

where σ_f is flexural stress, P is the load, r is the specimen radius, and L is the support roller spacing. It can be seen that for a given load P , the resulting stress in flexure acting as a tensile stress on the lower midpoint of the specimen will be reduced as the spacing L is reduced. This will result in higher compressive load at the roller surface to attain the same flexural stress, which may lead to failure at the support roller in compression prior to the flexural strength limit being reached.

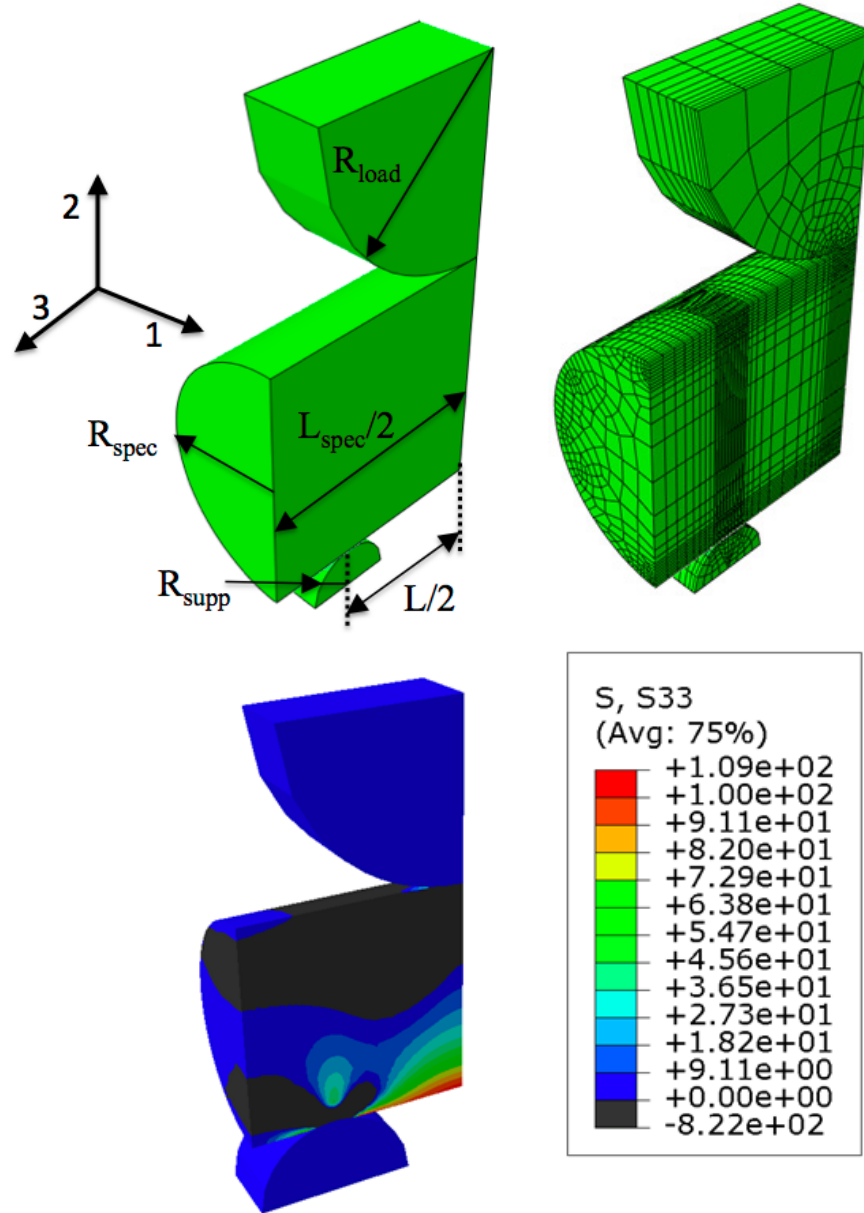


Figure 3. Finite element modeling of a three-point bend test on a cylinder with a 2-to-1 height to diameter ratio shows the desired buildup of tensile stress along the lateral tensor σ_{33} at the lower section of the specimen directly between the load rollers. Only half of the symmetrical configuration is shown.

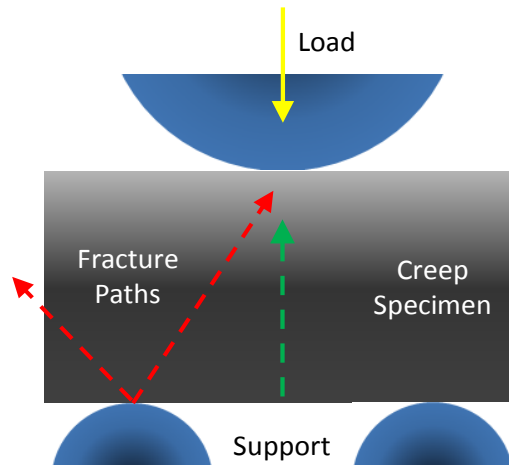


Figure 4. The common fracture paths in a sub-sized flexural specimen under three-point loading. The green arrow shows the desired fracture path due to flexural stress, while the red arrow show two directions of failure that initiate at the support roller contact point.

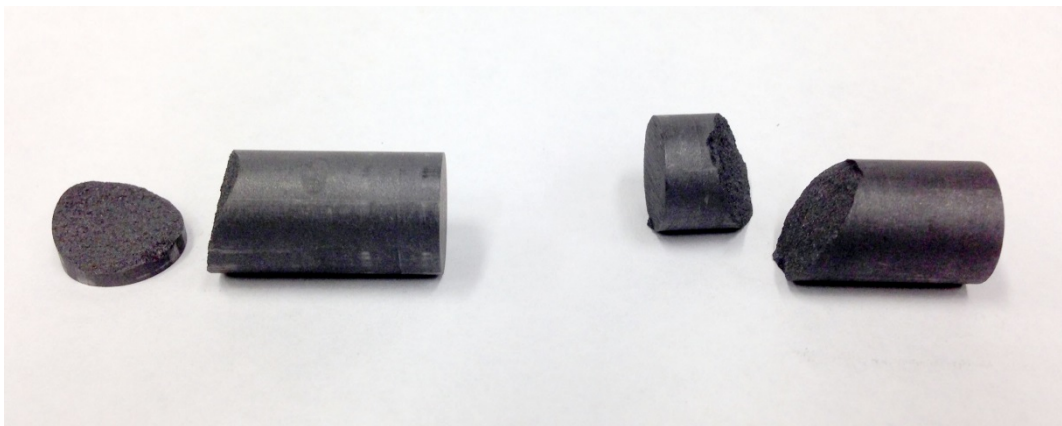


Figure 5. Examples of the fractures that initiate at the load roller contact point, as observed during the scoping study to determine the most appropriate configuration to facilitate reproducible failure in flexure. The left example shows compressive failure due to the support roller being too close to the outer edge; the right example shows compressive failure at the roller resulting from an inadequate margin between tensile loading at the lower midpoint and compressive stress at the roller contact point.

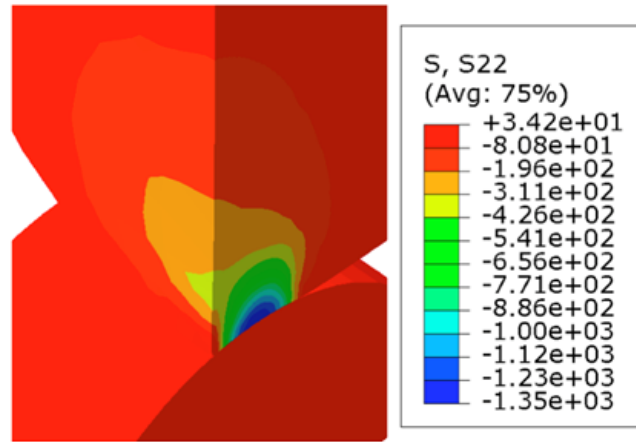


Figure 6. The simulated stress field around a roller-specimen contact point demonstrates the interaction of the stress with the free surface at the end of the specimen. The inability to accommodate this stress with surrounding graphite can lead to end failures of the specimen.

In the case of failure at the roller, Figure 7 demonstrates the effect that larger rollers have in reducing the contact compressive stress at the roller-specimen contact point. Despite the limited contact area between a curved roller support and an orthogonally-oriented cylindrical specimen, the roller size can have an effect on stress intensity and the stress field at the contact point. Larger rollers are therefore ideal for precluding compressive failure at the support roller. Larger rollers have an unfavorable effect on the test quality, however, in that the bending motion of the specimen under load is effectively shortened as the specimen begins to move inward around the curvature of the support roller, resulting in a reduced length between the support roller contact points and compromising the load vs. flexure stress relationship. Taking all practical measures to limit the support roller radius of curvature helps alleviate this test anomaly, a consideration for flexural testing that was previously identified and reported⁹ in the testing of ceramics. The ideal test, therefore, has a roller spacing as wide as will be allowable to preclude separation at the specimen ends with rollers as small as allowable while remaining sufficiently large so as to preclude fracture at the support roller surface. Fractures at the center of the specimen are an indication that the ultimate failure mode is in flexure, and consistent fracture in this region indicate that the test configuration is providing a valid measure of flexural strength based on the applied load at failure. In order to ascertain the most ideal three-point flexure fixture configuration, two distinct types of nuclear-grade graphite were selected for the scoping study test matrix – NBG-18 and IG-110. NBG-18 is the candidate graphite grade with the largest particle filler size and therefore the most susceptible to size effects in the limited geometry. IG-110 is a very fine grained graphite with high strength, and is therefore the most susceptible to fracture at the contact points owing to the high loads that it will accommodate prior to failure in flexure.

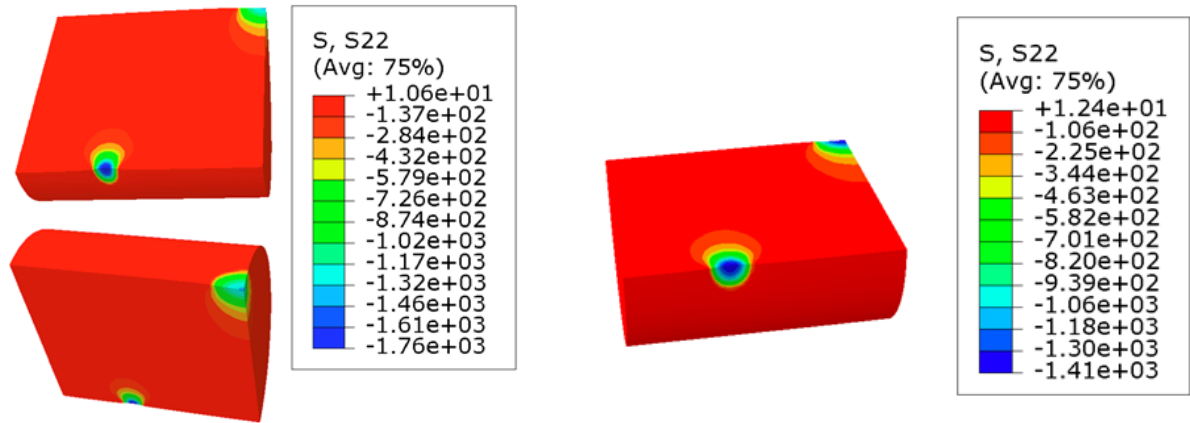


Figure 7. The reduction in stress due to larger roller diameters is shown by the magnitude of the stresses in the filed surrounding the contact with a 4.5 mm roller (left) and a 9 mm roller (right).

The final area of consideration for the mechanical testing of irradiated AGC graphite was the specimen containment approach. To this end, poly-based bags of different thicknesses up to 12 mils were an integral part of the test matrix and scoping analysis. Although strain values obtained through measured deflection is not a reportable property in flexural testing per the ASTM standard, the ability to collect this data for potential future evaluation is an important consideration. The Baseline flexure data has recorded strain measurements for all flexural tests run in that program, and so for future comparison purposes minimizing the strain offset due to the compression of the containment bag is therefore an additional area for investigation. Understanding what level of applied load results in full compression at the contact points will allow the true strain specific to the graphite while being loaded in flexure.

Based on the results and observed fracture of the specimens in the scoping study, the final configuration determined to be ideal for the cylindrical AGC specimens is shown in Figure 8. 9 mm support rollers with centers spaced at 16 mm was not only robust enough to ensure that a technician tasked with centering the bagged specimens on the support roller assembly could be accomplished with a reasonable degree of accuracy, but also demonstrated fracture at the midpoint of the specimens for each of the graphite grades being evaluated. The containment considered ideal for the testing was polyurethane material 6 mils in thickness, the utilization of which demonstrated no tearing at the contact points over the course of the test regardless of the applied load that facilitated fracture of the individual specimens.

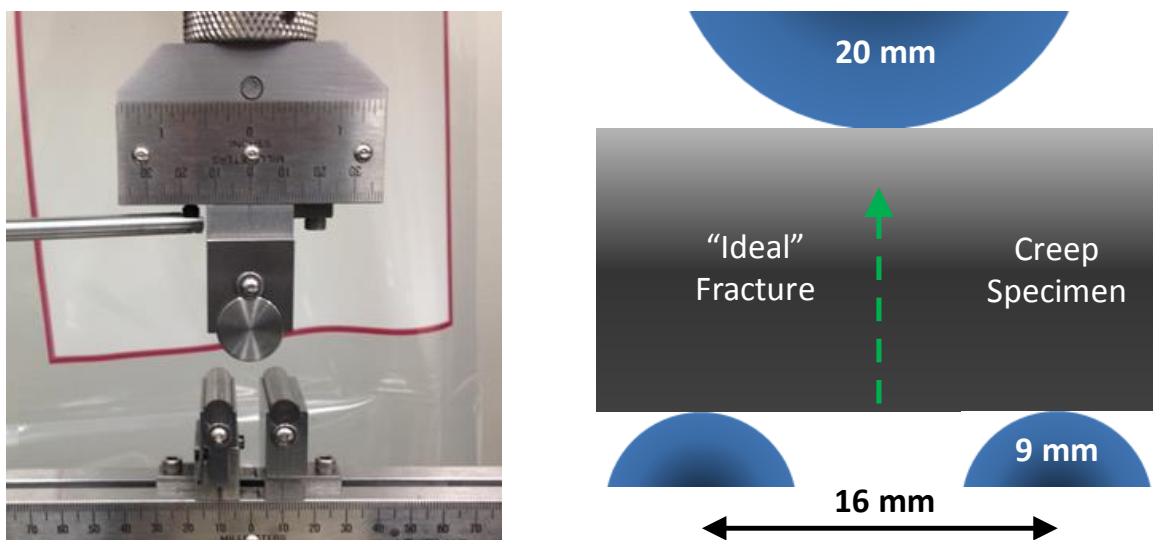


Figure 8. The final setup as run for the scoping study (left) resulted in fracture at the maximum tensile stress due to flexural loading, resulting in fracture at the midpoint of the specimen as shown schematically (right).

2.3 Experimental Results

Testing of specimens in the Carbon Characterization Laboratory (CCL) was initiated with the unirradiated sister specimens in order to familiarize the radiological controls and test technicians with the procedure prior to handling irradiated specimens and to ensure that the Bluehill™ software output captured the data in a manner consistent with the baseline test data for four-point flexure testing. Figure 9 shows the test setup at the load frame in the CCL. The actual testing protocol requires a coordinated effort by multiple people. One test technician is properly outfitted to handle and load specimens into the load frame under the supervision of a Radiological Controls technician. A third qualified technician handles the operation of the load frame from outside the Radiological Buffer Area (RBA). The hands-on coordination of the team is shown in Figure 10. The initial testing of radiological specimens¹⁰ was carried out with two standard AGC creep specimens from the AGC-2 experiment, one PCEA specimen and one NBG-17 specimen. Both were chosen to provide a direct comparison with unirradiated PCEA and NBG-17. The relative load-deflection curve for a specimen of NBG-17 is shown in Figure 11.

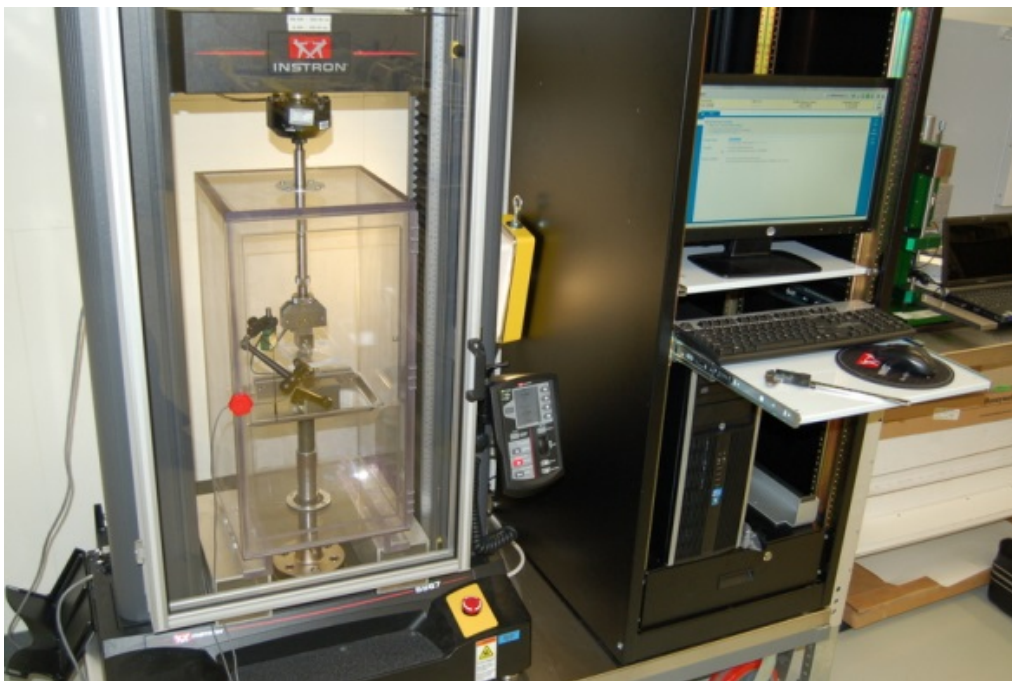


Figure 9. The load frame in the Carbon Characterization Laboratory.

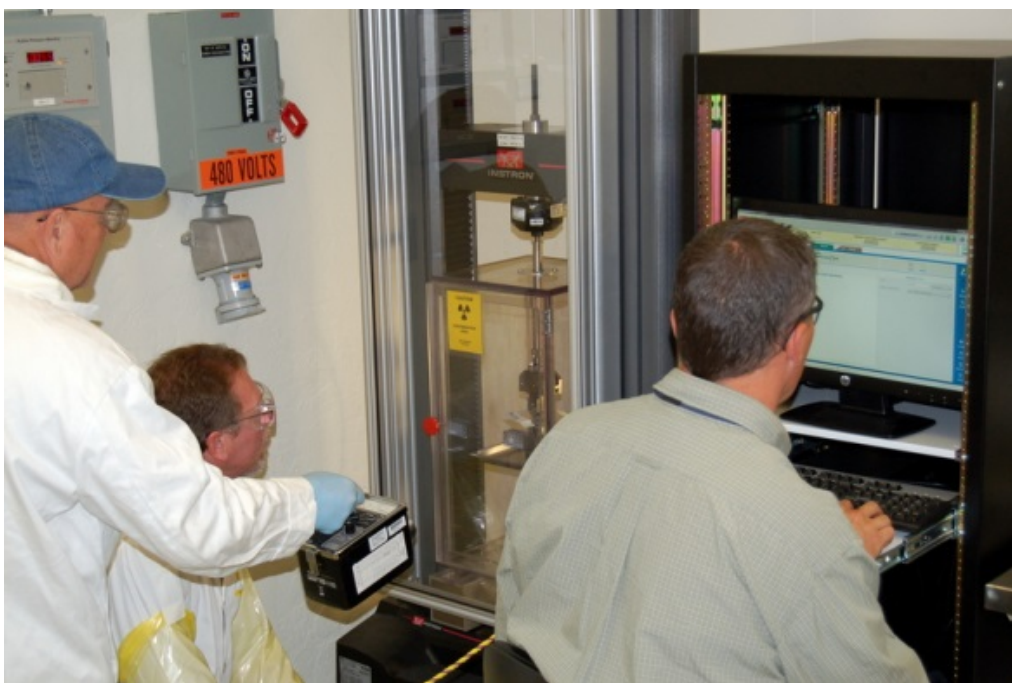


Figure 10. A coordinated effort between a frame operator (right), a technician who handles and loads the irradiated specimens (center), and radiological controls monitoring (left) ensure an effective test protocol for AGC specimens.

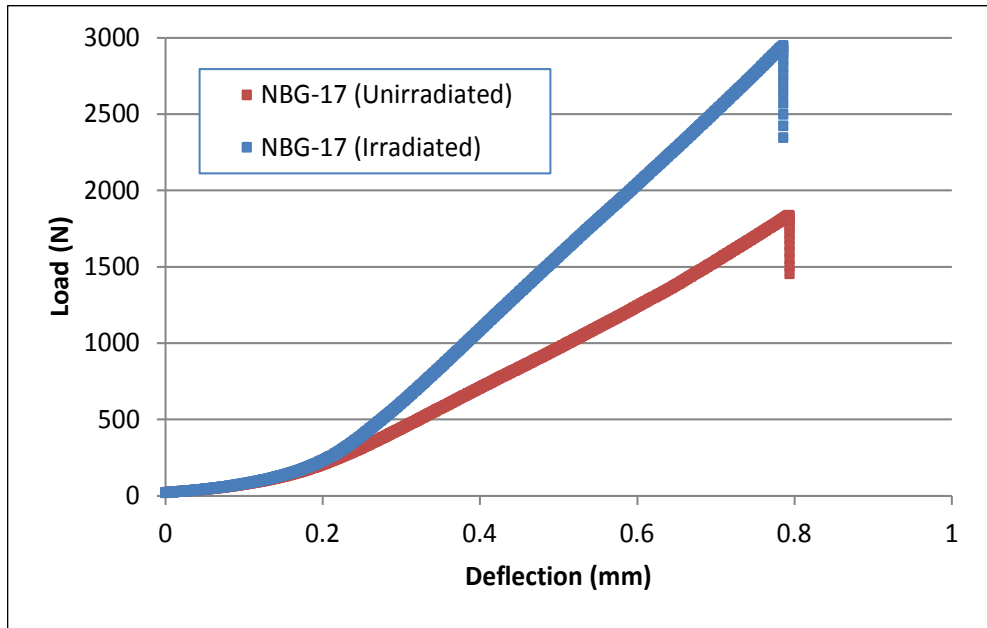


Figure 11. A representative load-deflection curve for the initial mechanical testing on AGC-2 specimens shows the increase in both strength and modulus following irradiation as compared to the unirradiated sister specimen. This particular sample was NBG-17.

The commencement of the full range of irradiated AGC-2 specimens revealed that the test fixture configuration may not be adequate for stronger nuclear grades of graphite. As shown in Figure 10 for the fracture of specimens in flexure, the irradiation of specimens results in an increase not only in effective modulus but also in ultimate strength. Despite the fact that the scoping study demonstrated reliability in flexure mode fracture for IG-110, the initial testing on the irradiated AGC-2 IG-110 and IG-430 specimens demonstrated fracture that initiated at the support roller surface, clearly revealed by a diagonal fracture pattern between one of the support rollers and the central load roller (Figure 12). The reason for this anomalous fracture mode was determined to result from two potential conditions. One was fracture at the support roller due to the increased point loading at the support roller surfaces resulting from the increased load being applied during the test to enable failure of the stronger irradiated grades. The other was potentially due to lateral deflection of the load roller assembly due to the long shaft between the load cell and the load roller. Any deflection in the upper assembly would unbalance the load distribution between the load rollers and lead to a larger stress concentration at one support roller surface, resulting in the aforementioned fracture initiation at one of the support roller contact surfaces.

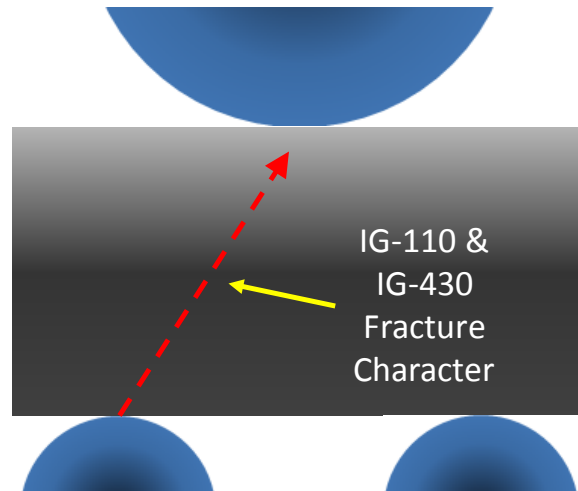


Figure 12. The fracture in the stronger fine-grained graphite grades indicated that the irradiation effects reduced the effectiveness of the approved fixture configuration with regard to preventing fracture initiation at the support rollers.

In order to alleviate the potential for both conditions, several significant modifications were made to the flexure fixture prior to re-commencing test activities. First, the load roller shaft was shortened and the load contact surface was changed from a roller assembly to a rigid curved surface, which is appropriate for three-point flexure testing as no lateral displacement of the specimen is allowable at the midpoint. These two changes reduce the opportunity for lateral deflection of the load surface from the desired midpoint position, ensuring the load is equally counteracted at the support rollers. The second modification was to increase the support roller diameter to a maximum value of 12 mm. Figure 13 demonstrates the reduction in the σ_{22} (compressive) tensor values based upon an increase in roller diameter from 9 mm to 12 mm, which represents the largest practical diameter for the support roller assembly based upon the fixture's support system and desired roller spacing of 16 mm. The modified flexure fixture is shown in Figure 14.

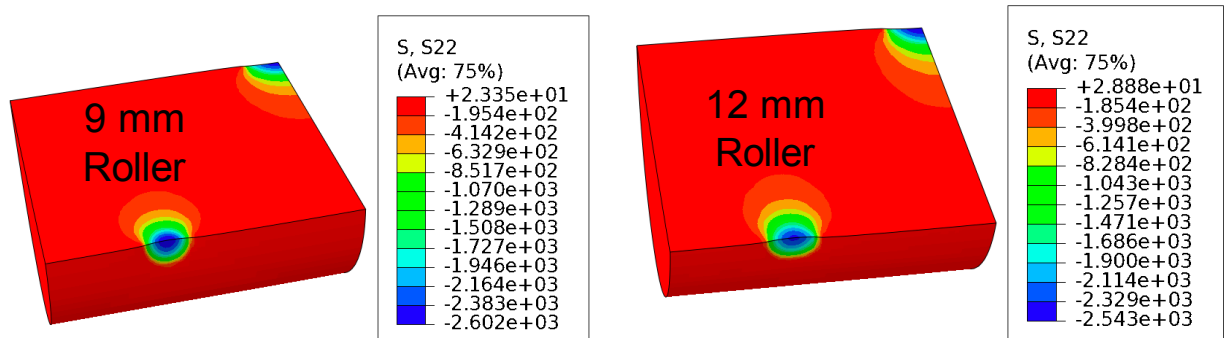


Figure 13. An increase in roller size from 9 mm to 12 mm provides a further reduction in compressive stress at the roller contact point, reducing the likelihood for support roller fracture initiation.

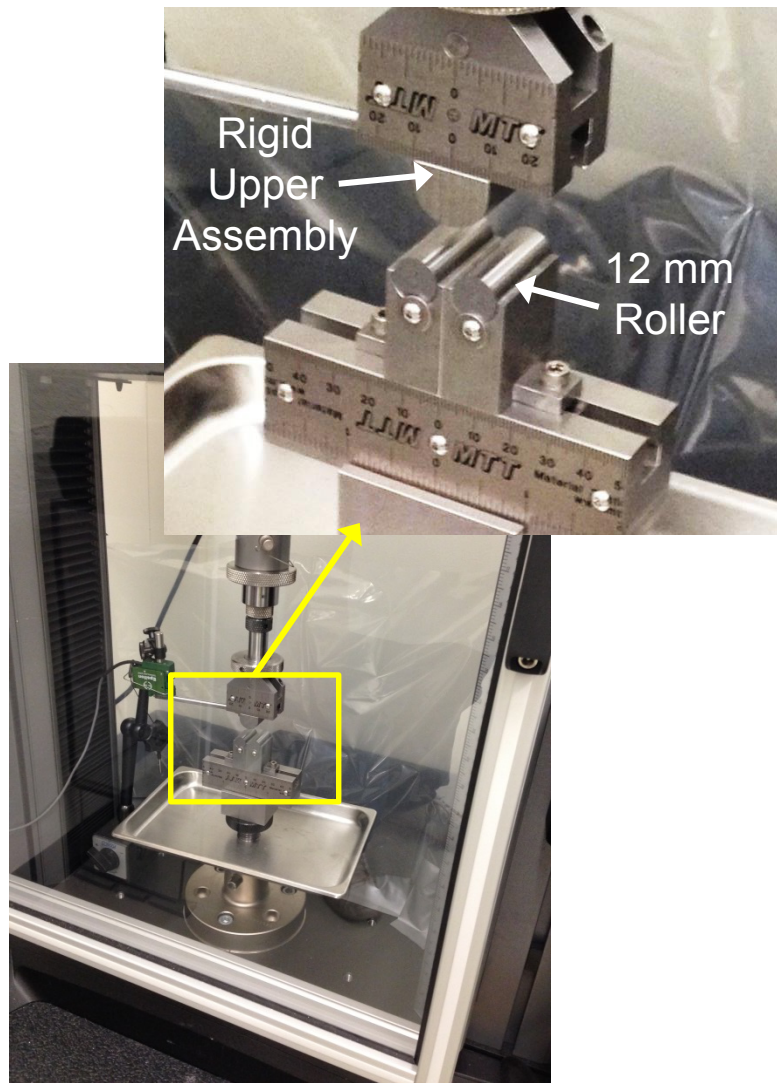


Figure 14. The modified flexure assembly utilizes a shortened upper (load) shaft to minimize lateral deflection, a rigid load contact radius rather than a roller, and larger 12 mm support rollers. The modified configuration was effective at reducing roller contact failure.

Testing recommenced on the remaining IG-110 and IG-430 graphite specimens from the AGC-2 experiment, and the observed fracture for each of the grades indicate that the changes were effective at alleviating the diagonal fracture pattern. A comparison of the limited amount of test data between the initial and unmodified fixtures indicate that any change to the measured flexure strength is within the data scatter common to graphite mechanical testing, but the fixture configuration will remain in the modified setup in order to ensure that the data being collected is more reflective of failure in a true flexural mode. Table 1 is a listing of all of the specimens that were tested for the AGC-2 mechanical testing effort, including the sister specimens that provided a means for more direct comparison of pre- to post-irradiation effects.

Table 1. The specimens taken from the un-stressed AGC-2 inventory for mechanical testing, along with a selection of sister specimens to provide comparative strength values.

Unirradiated (Sister) Specimens					
<i>Grade</i>	H-451	PCEA	NBG-18	IG-110	IG-430
	CW06 01	DW7 02	BW6 01	EW01 01	FW12 02
	CW08 02	DW8 01	BW6 02	EW11 01	FW12 03
	CW12 01	DW9 01	BW8 03	EW11 04	FW12 04
	CW9 01	DW9 02	BW9 02	EW12 01	FW13 02
	CW9 02	DW9 03	BW9 03	EW13 02	FW13 04
	CW9 03		BW9 01	EW13 03	FW14 04
				EW13 04	
Irradiated AGC-2 Specimens					
<i>Grade</i>	H-451	PCEA	NBG-18	IG-110	IG-430
	CW1 03	DW10 03	BW10 02	EW02 02	FW02 01
	CW11 02	DW13 03	BW14 02	EW05 02	FW02 04
	CW13 01	DW16 04	BW3 02	EW08 02	FW05 02
	CW2 02	DW11 02	BW11 02	EW02 04	FW06-01
	CW3 03	DW14 02	BW15 02	EW04 01	FW08 03
	CW5 01	DW17 04	BW4 02	EW05 04	FW09 02
	CW10 02		BW11 01	EW08 04	
	CW13 02		BW15 01	EW02 03	
	CW4 01		BW4 01	EW05 03	
				EW08 03	

With the emphasis for evaluating the performance of nuclear grade graphite being on probabilistic property data, specific strength performance is analyzed with regard to distributions of data rather than average or otherwise nominal scalar values. Owing to the consistently high goodness-of-fit values for Weibull distributions of graphite properties when compared to other distribution types, Weibull-based data distributions will be the method for describing the results of the mechanical strength properties and the means for comparison with the Baseline Graphite Characterization data sets. The specific distributions of data from the individual test specimen populations will therefore emphasize cumulative probability density functions $F(x)$ according to the Weibull relationship:

$$F(x) = 1 - e^{-\left(\frac{x}{\alpha}\right)^{\gamma}}$$

In this two-parameter relationship, x is the individual measured property, α is the associated scale factor below which 63.2% of the values from measured data set fall, and γ is the shape parameter describing the slope of the cumulative function. From a comparison standpoint, the scale factor provides a scalar, or characteristic, strength value that is representative of the entire distribution. The shape parameter, or slope of the distribution, provides an indication of the overall variability – a relatively steep slope indicates a lesser amount of variability than does a shallow slope quantified by a lower shape parameter. The two-parameter Weibull distribution is presently the only statistical analysis technique that is specifically adopted as an ASTM standard (ASTM D7846-12)¹¹ for the evaluation of graphite

mechanical properties. While evaluations will persist with regard to investigating the merits of other distribution types with the goal of providing the most accurate model for property distribution probabilities, the Weibull distribution will continue to be utilized as the main tool for presenting data sets for comparison. The discussion relating the AGC-2 mechanical test data with the more comprehensive Baseline property datasets will be based on comparisons of Weibull distributions between the test results.

As was shown in Figure 10, it is expected that an increase in measured mechanical strength will result from the AGC-2 irradiations. In order to provide context for the increases in strength, distributions for the unirradiated sister specimens of the five graphite types (Figure 15) show the characteristic flexural strength, as determined by the Weibull scale parameter, increasing in order as H-451, PCEA, NBG-18, IG-110, and IG-430. At the lower end of the flexural strength scale are the two extruded grades, H-451 and PCEA, while the fine-grained isomolded grades IG-110 and IG-430 are at the upper end. NBG-18, in the middle of the relative scale, is a relatively large-grained vibration-molded grade. The distributions are relatively close in variability as well, with the exception of NBG-18, as reflected in the similar shape parameters. A further evaluation of this large relative level of variability will be examined in a later section of this report. The results of the irradiated AGC-2 specimens that correspond to the sister specimen grade and sub-blocks (Figure 16) show a very similar trend, with the same increasing order of relative strength and a similar large level of variability in NBG-18 when compared to the other grades. The individual Weibull cumulative density function plots for each of the grades, comparing the unirradiated to irradiated flexure strength data, are shown in Figure 17. The jump in flexural strength from the AGC-2 exposure ranges from approximately 15 MPa to almost 30 MPa based on a comparison of the respective scale parameters. The scalar quantification of these strength increases are shown in Figure 18 and Table 2. Because the values listed are representative of a distribution of data, there are no applicable “error” bars to indicate how tight the distribution is around those scalar values. This specific quality underscores the importance of considering both the scale and shape parameters from the Weibull distribution in the same manner than a “normal distribution” requires a consideration of both the mean value and standard deviation in order to fully describe the data being evaluated.

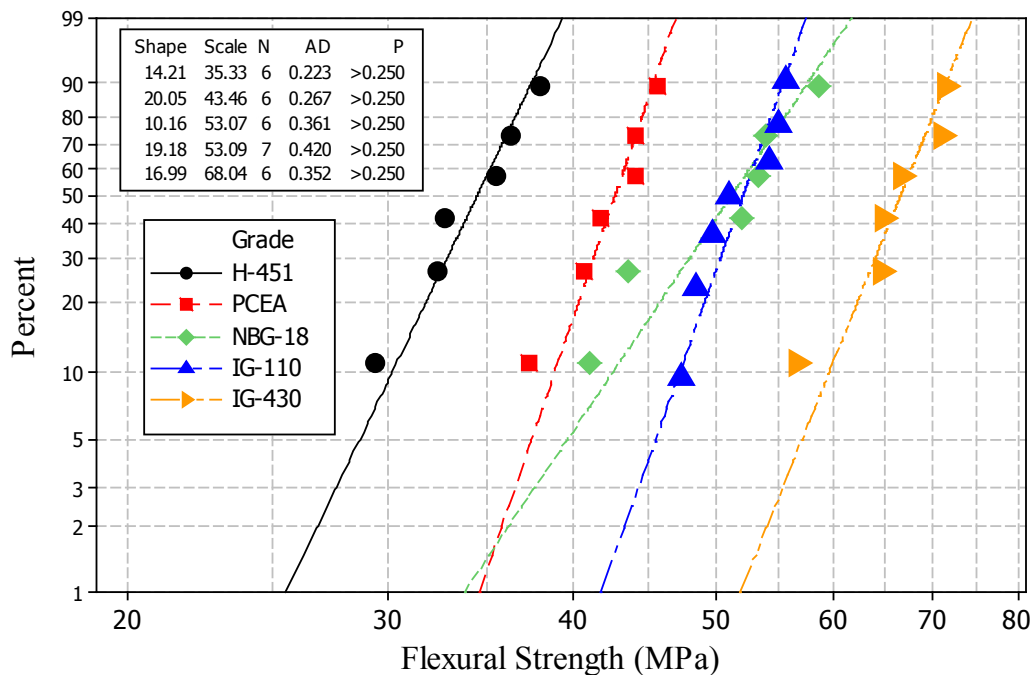


Figure 15. Weibull probability density functions for flexural strengths of the unirradiated sister specimens show the comparative strength levels between candidate graphite grades.

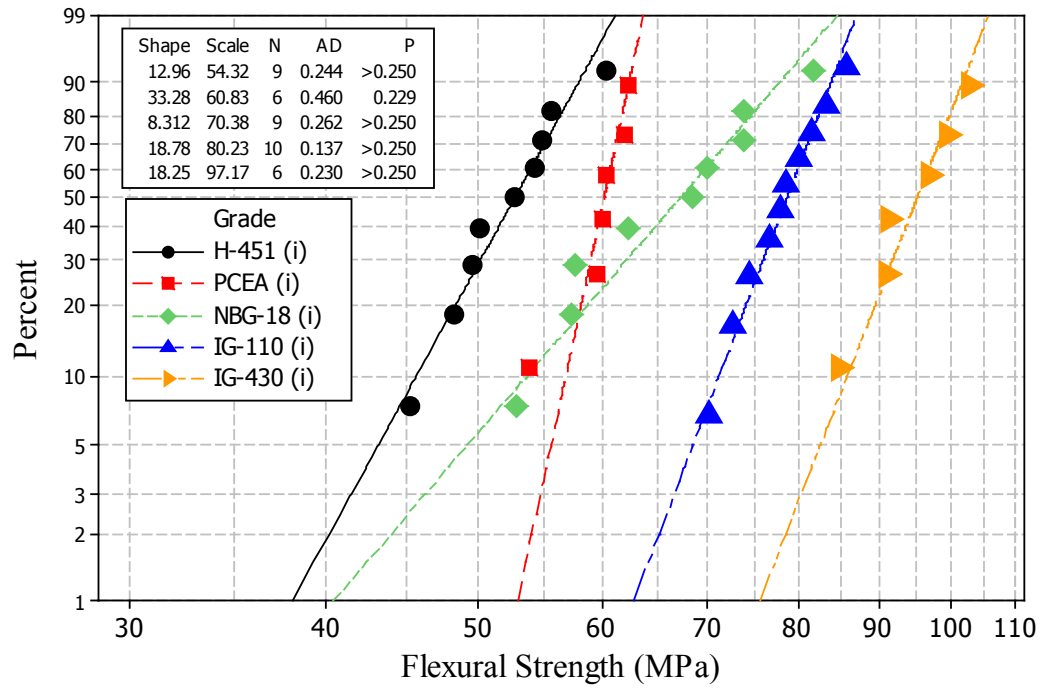


Figure 16. The irradiated AGC-2 strength distributions show a similar trend in relative strengths between grades, along with the expected increase in values following the AGC-2 exposure.

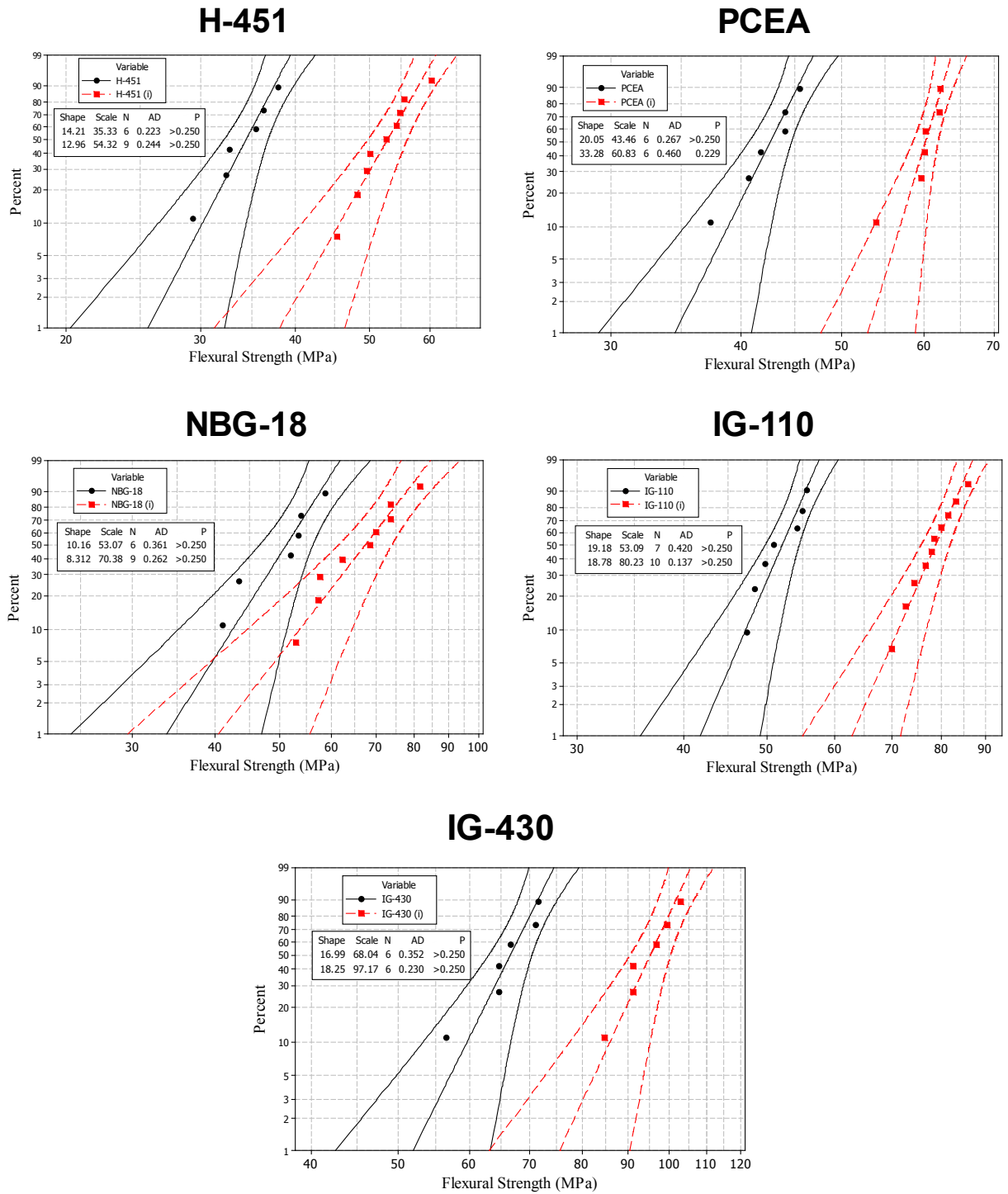


Figure 17. The individual shifts in strength for each of the candidate grades between the unirradiated sister specimens and the specimens irradiated in AGC-2.

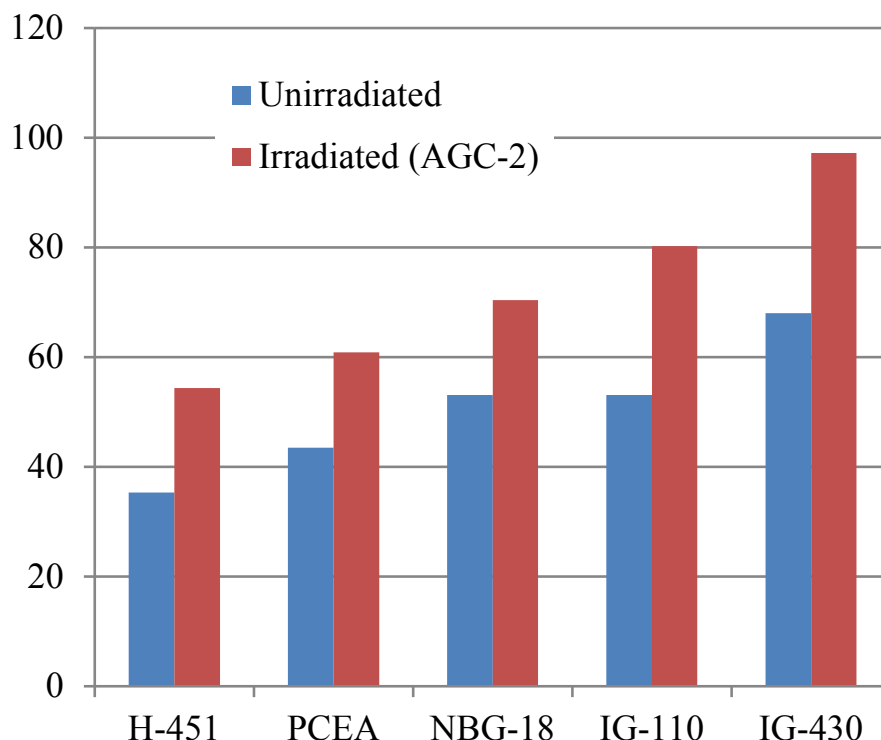


Figure 18. Quantification of the strength increases based on the Weibull scale factors shows the measurable increase in representative flexural strengths following irradiation.

Table 2. The listed Weibull scalar values for comparison between the tests. The comparison between unirradiated sister specimens in three-point bending differs significantly from unirradiated specimen testing on Baseline specimens in four-point bending.

Flexural Strength (Mpa)			
	Unirradiated	Irradiated (AGC-2)	ASTM 4-Point
H-451	35.33	54.32	
PCEA	43.46	60.83	29.50
NBG-18	53.07	70.38	28.42
IG-110	53.09	80.23	36.55
IG-430	68.04	97.17	

3. DISCUSSION

A full analysis of the AGC-2 mechanical strength data must include more than the limited number of data points for each of the grades in both the irradiated and unirradiated conditions in order to comprehensively capture the inherent variability in nuclear grade graphites. To this end, the Baseline Graphite Characterization data can provide a highly detailed indication of this level of variability in order to increase the resolution of the distributions being generated from the individual AGC experiments and provide a more accurate probabilistic determination of grade-specific properties and performance. As was noted earlier, there is a significant deviation from the recommended height-to-diameter ratio for the three-point bend approach to mechanical testing of AGC specimens and this deviation must be accounted for when fully analyzing the resulting data. As shown in Figure 19, the flexural strength data from

ASTM-based four-point bend testing are considerably lower for the three grades, PCEA, NBG-18, and IG-110, with pertinent Baseline data that were also part of the AGC-2 experiment (H-451 is a legacy grade for comparison and not considered one of the candidate nuclear grades; IG-430 is not expected to include a large amount of Baseline testing due to its relatively low consideration as a candidate grade at this time). During the execution of individual tests, the ASTM standard specimens tested in four-point flexure are stressing a much larger effective volume of material due to the shape and geometry of both the fixture and the specimens themselves. Being that they are entirely unconstrained by Advance Test Reactor test train limitations, the specimens can be machined to whatever size and geometry is prescribed by the pertinent standards, and the four-point test configuration produces a tensile load peak that stretches across the entire section of the specimen below the two load rollers. As such, the volume under peak stress and the available flaw population inherent to graphite allows a more representative capture of “limiting” flaws that initiate fracture. This phenomenon is aptly illustrated by the largest variability in values being demonstrated by NBG-18, which has a grain size (and directly related flaw population scale) of 1.6 mm, which is twice the size of the extruded grades and two orders of magnitude larger than IG-110 and IG-430. The flaw in the microstructure that results in fracture under the applied stress is therefore highly variable, as the critical stress field is on the same relative order as the grain size of NBG-18. The graphite will concomitantly exhibit strength properties that vary from those that reflect a relatively large flaw in relation to the volume of the stress field (resulting in a low strength value) to those that do not capture the nominally larger flaws in the volume under stress (resulting in elevated measured strength levels). The size effect on measured flexure strength due to flaw population vs. volume under stress can be quantified via the scale parameter in a two-parameter Weibull distribution. For Baseline specimens tested in standardized four-point flexure¹² for PCEA, NBG-18, and IG-110, those values are 29.50, 28.42, and 36.55 MPa, respectively, based on the number of specimens tested thus far in the program. The difference in measured strength level between the non-standard three-point test and the ASTM-based four-point test is reflected in three-point measured values that are more than double those of the four-point test on approved geometries, despite the fact that they ostensibly reflect the same mechanical property. This disparity is considerable, but the property value distribution that is most pertinent to the small sample populations of the AGC experiments is still most accurately reflected by the standard specimens, in which not only is a much larger sample population being tested, but the stress-induced fracture of the individual specimens much more accurately captures the limiting flaws that determine the strength levels in that particular test. For this reason, the distribution factors captured in the Baseline datasets provide distribution information that can appropriately be applied to the measured AGC irradiated and unirradiated distributions in order to provide some context into the test limitations and whether or not the distributions from the AGC experiments are appropriate, and, more importantly, provide a means to more accurately capture the corrected graphite distribution in a manner that can facilitate probabilistic property determinations.

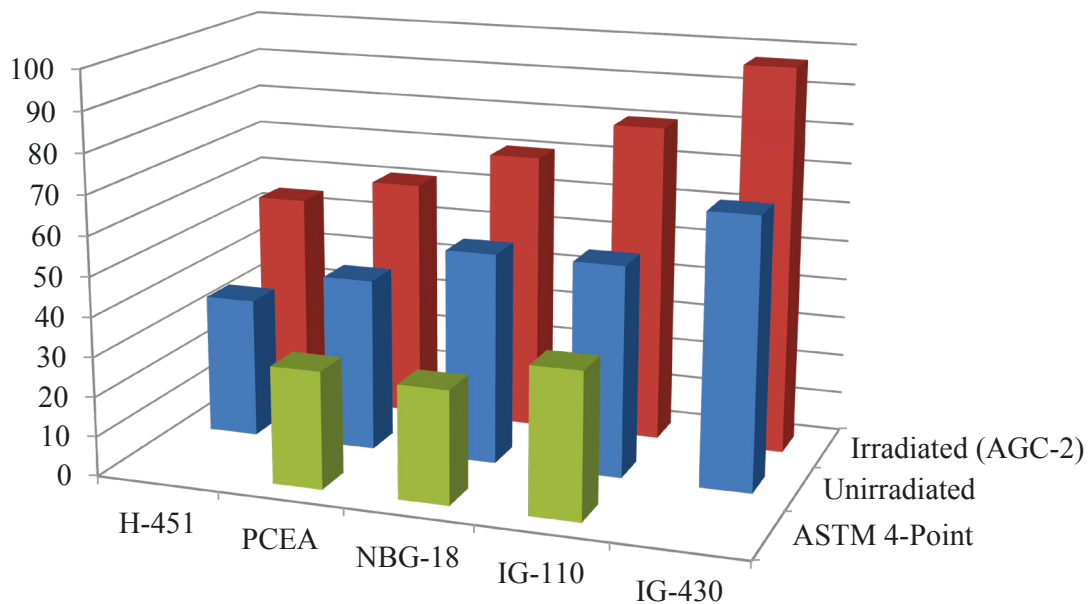


Figure 19. Comparisons between both the irradiated and unirradiated three-point test results and the standard four-point bend results from the Baseline program indicate significant differences in measured values. Integration of the trends seen in datasets must consider not only external effects such as temperature and dose but also effects due to the specific test approach.

Figure 20 shows the shift in Weibull distributions between the four-point flexural test results for NBG-18, as collected from standard ASTM-sized specimens and the AGC-2 irradiated and sister specimens. As was described in the previous section, the limited amount of volume under stress for the three-point bend specimen will have a large effect on the variability in data for a larger-grained grade such as NBG-18. Although this could be corrected to some extent through the collection of data on a larger sample population, it is considerably more effective with regard to resources to gain insight into the appropriate variability through a comparison with Baseline data. As the shape parameters demonstrate, the variability in data for flexural strength from a large population of standard test results has a much higher value as reflected by the slope. The shallower slope of both the unirradiated sister specimen results and of the irradiated AGC-2 specimens indicates that the probabilistic flexural strength data that can be ascertained from this data alone is overly conservative. As more of the AGC data is compiled through the completion and post-irradiation examination and testing from the other experimental runs, a more reflective overall distribution of strength data can be compiled that takes into consideration not only the translation of data between pre-irradiation and post-irradiation examination with regard to temperature and dose, but also the correction in variability based on the execution and compilation of standardized strength distributions. From the data collected thus far in the program, the irradiated NBG-18 data shows a distribution that should be corrected to reflect less variability.

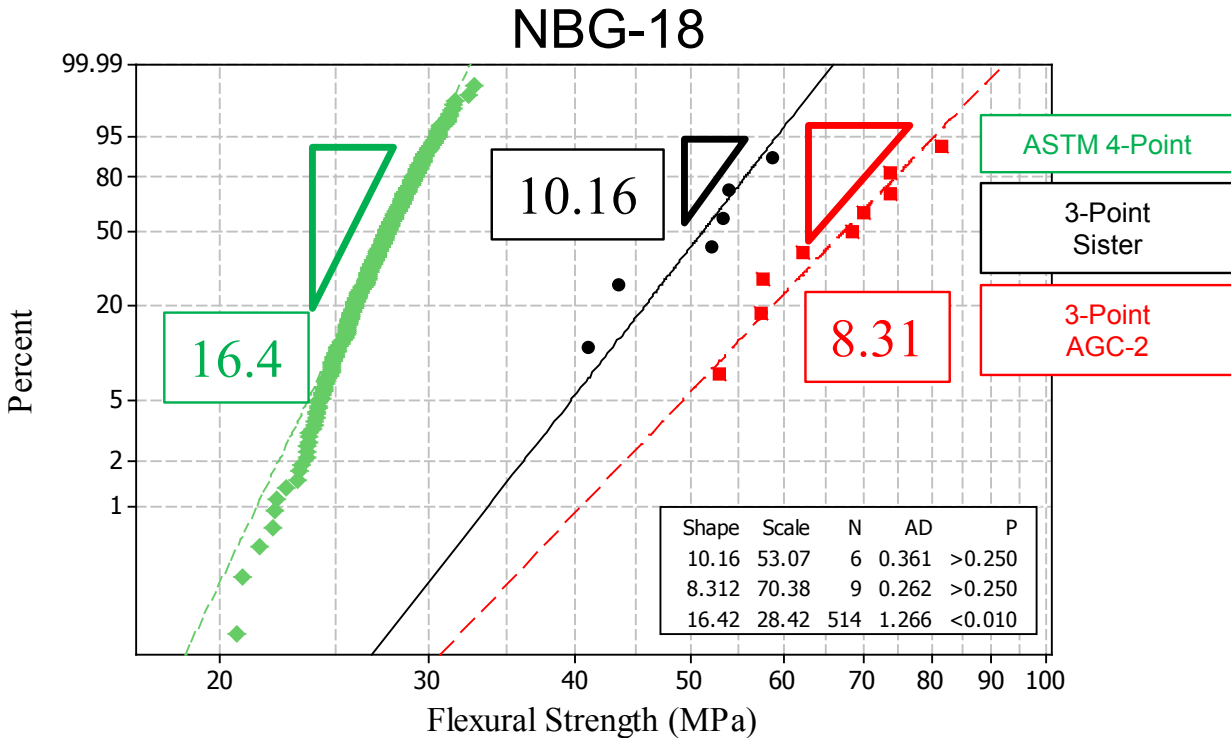


Figure 20. A comparison of flexural strength results for NBG-18 indicates considerably less variability (as evidenced by the higher Weibull shape parameter) for the comprehensive Baseline data set. The variability in AGC-2 strength data conservatively exhibits higher variability.

A very different effect is seen in the comparison of the PCEA data between the different tests and conditions. While the size effect for homogeneously distributed flaws will be less deleterious to the PCEA data, what will likely not be captured in the limited AGC test data and stressed volumes is the larger disparate flaw population that greatly increases variability across large PCEA specimen populations. As was described in INL/EXT-33120 “Initial Comparison of Baseline Physical and Mechanical Properties for the VHTR Candidate Graphite Grades,”¹² PCEA is prone to relatively large flaws and regions of lower density in certain prevailing areas in the full-sized billets. These flaws are captured in the comprehensive Baseline results, but are likely not captured in the specimens extracted from single sub-blocks from the original billets for the AGC experiments. As shown in Figure 21, the variability in the unirradiated sister specimens is extremely small and is smaller still for the irradiated specimens from the AGC sample population. Compared to the standard four-point flexure strength distribution, the variability in the AGC data does not reflect the variability seen in inter- and intra-billet populations. The extraordinarily tight distribution of PCEA AGC-2 data is an area for further detailed investigation; it may reflect an unusually high homogeneity in the sub-block from which these specific specimens were extracted, or it may provide insight into more complex microstructural phenomena that occur during irradiation. It is likely both, in that the sister specimen distribution shows considerably higher variability than the irradiated specimen distribution. From a microstructural standpoint, the irradiated response of PCEA could well be an inherent flaw “crack-tip” blunting effect or pore closure in the material that is particularly beneficial to the fracture properties following irradiation. From the limited data available at this point in the experiment, it will be difficult to expand upon the potential for such mechanisms. The results of the additional AGC experiments will help clarify whether this behavior is anomalous or a very real reflection of the response and the basis for a more thorough mechanistic

understanding. What is clear at this point is that the AGC-2 data does not accurately reflect the amount of variability in PCEA, and the integrated distribution will likely show a wider distribution that is representative of the Baseline shape parameter for the purposes of evaluating probabilistic strength values.

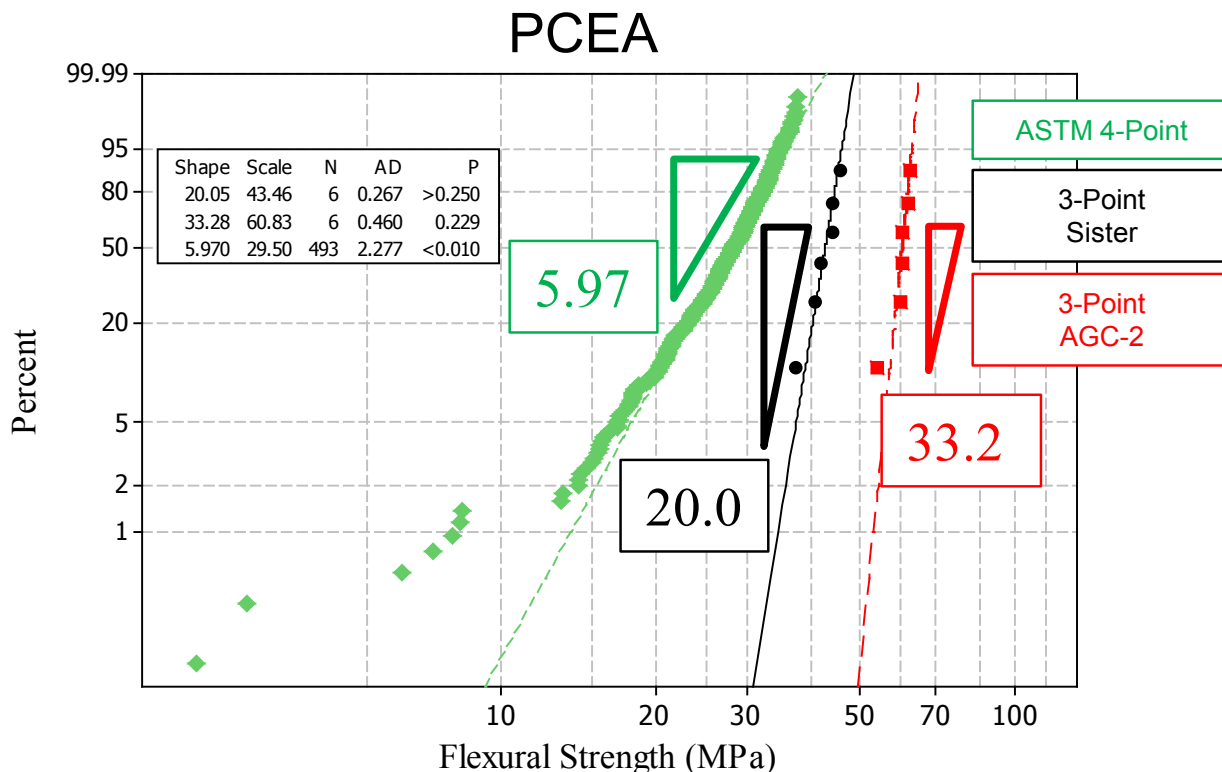


Figure 21. The comparison of flexural strength results from PCEA indicates that the appropriate level of inherent variability in the graphite grade is not reflected in the AGC-2 strength distribution. The overall probably strength distribution for irradiated properties must consider this higher level of variability.

Between the NBG-18 and PCEA strength value observations and comparisons is that for the IG-110 (Figure 22), in which the Baseline database is much less complete than that of the other two grades but indicates a slightly higher level of variability than that of the unirradiated sister specimens or the AGC-2 irradiated specimens. With the shape parameters being relatively close, there is a much higher likelihood that the data obtained during the AGC experiments will not require a large level of data distribution manipulation in order to provide a high degree of confidence in the probabilistic irradiated mechanical response properties.

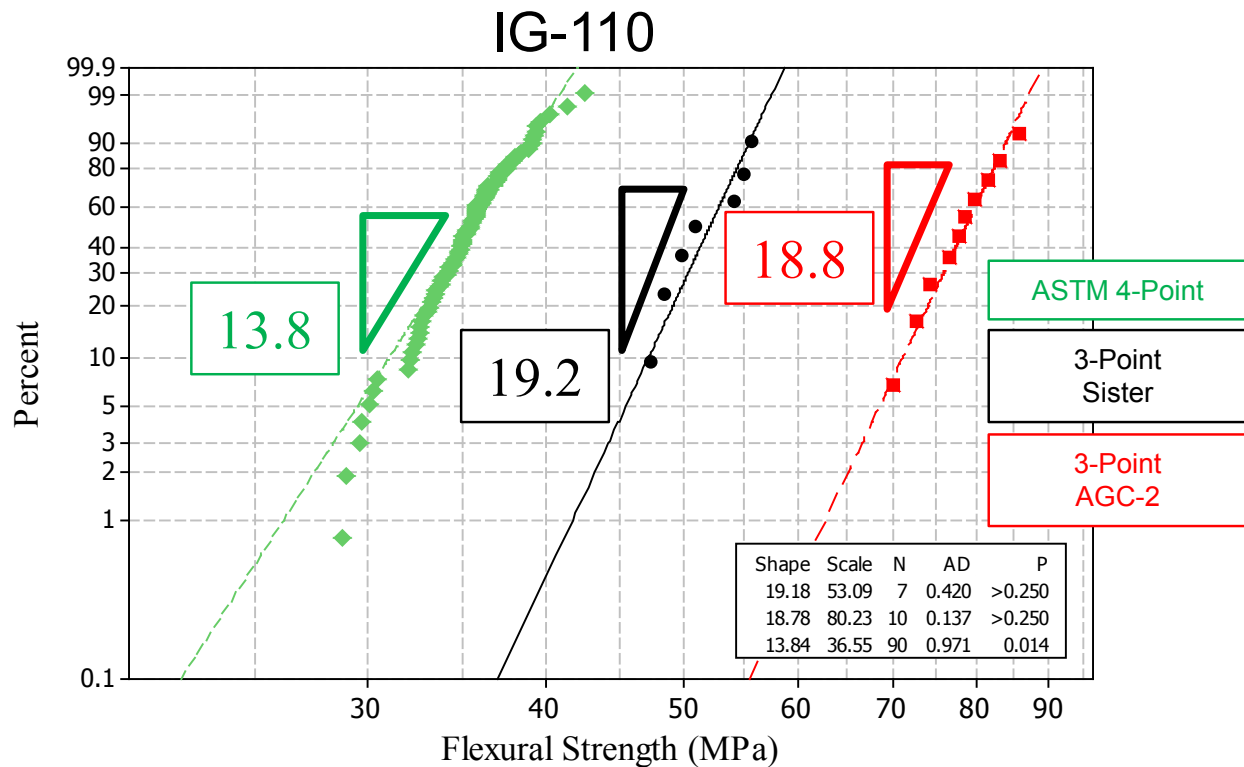


Figure 22. IG-110 exhibits a level of variability in measured flexural strengths that is comparable between the different test and conditions. The AGC-2 strength results show slightly less variability than should be expected based on the larger Baseline data level of inherent property variability.

In summary, the comparison of the Baseline datasets and AGC-based datasets relies on several qualities of the distributions. The translation in values between the sister specimens and the irradiated AGC specimens provides a direct correlation between pre- and post-irradiation properties based upon specimens taken from the same relative positions within a billet and the exact same test configuration and associated geometry. The ultimate distribution in data for the irradiate graphite must be corrected by the shape factors determined in the Baseline Graphite Characterization program, in which not only are much larger populations from a wider range of graphite billets and internal locations being evaluated, but tests are being run in strict adherence to ASTM International standards under conditions that are unencumbered by the size and geometrical constraints placed on AGC-based experimental specimens.

While the breakdown of the limited data available into smaller subgroups will not necessarily provide compelling evidence for specific conclusions, some indication can be gained as to the effects of different radiation doses and temperatures on the AGC-2 grades under test. While a full accounting of the dose and temperature effects will gain considerable detail through data gained from all of the AGC experiments compiled into comprehensive groups, there was a degree of variability identified in the dose and temperature parameters planned for the AGC-2 experiment. A peak in the flux profile near the core centerline resulted in elevated dose and temperature levels when compared to the upper or lower sections of the test train. While further analysis is ongoing, Engineering Calculation and Analysis Reports (ECARs) indicate that the dose in AGC-2 ranged from approximately 1.8 dpa to 4.6 dpa,¹³ while the temperature ranged from 550°C to 720°C.¹⁴ Since the cross-section of AGC-2 specimens removed for mechanical testing included distinct groups from “high” dose and temperature regions and “low” dose and temperature regions, preliminary comparisons can be made even with the limited data available. Figure 23 shows example comparisons of PCEA and IG-430 graphite, in which the high and low value regions from

within a single experiment can show some variability in the distributions. Although there is considerable overlap in the confidence intervals between the distributions, the higher dose specimens exhibit the expected higher scale parameters in their respective distributions. Logical groupings of data based on the results of dose and temperature analyses from subsequent AGC experiments and testing will help sharpen these differences in the established property distributions and extract the individual dose and temperature effects.

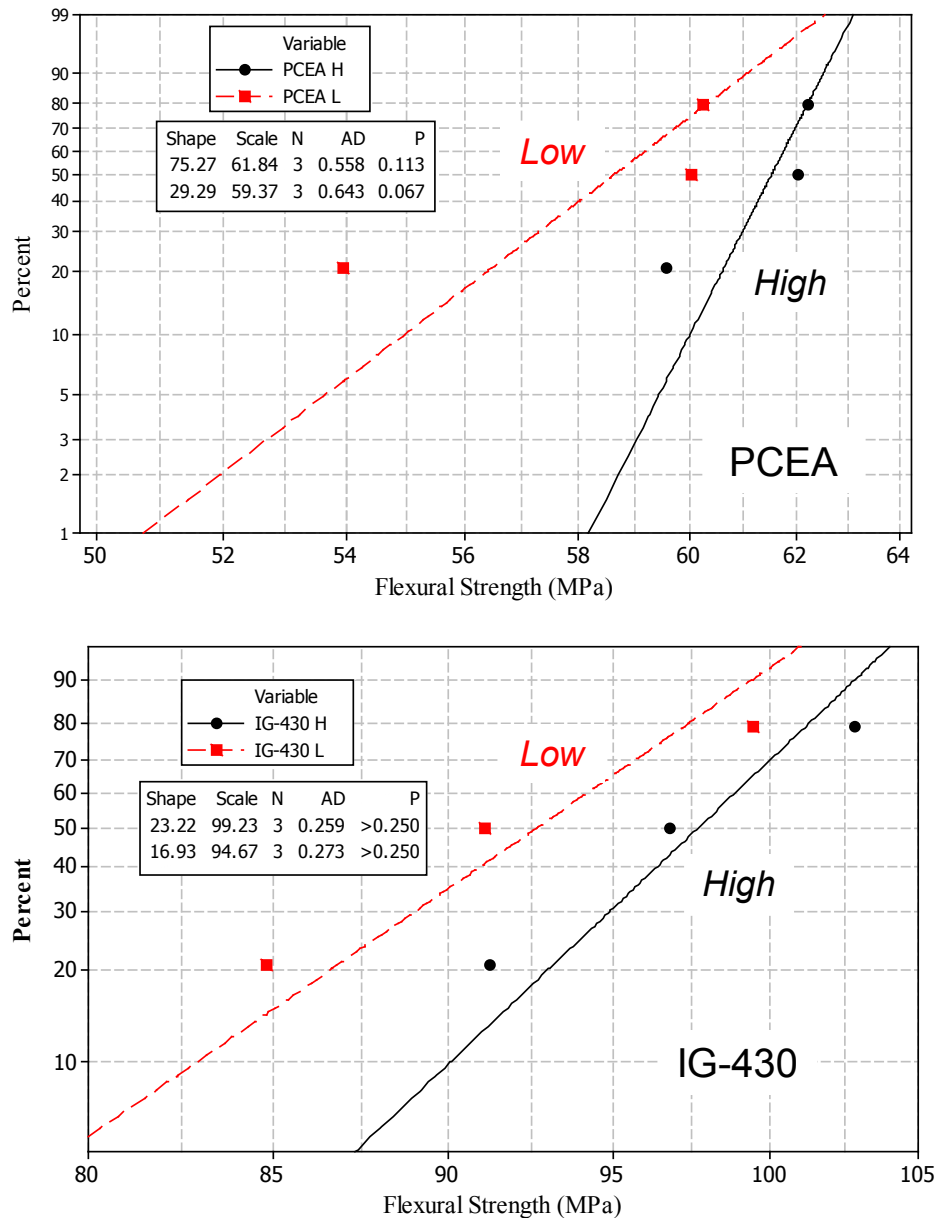


Figure 23. Preliminary analysis suggests that a measurable peak in the flux profile at the core midpoint resulted in higher dose and temperature exposure to specimens near the center of the test train. Examples of grouping the results by “high” and “low” dose and temperature values based solely on position in the core indicate that a difference in final properties does exist.

4. FUTURE WORK

Based on the results of the comparison data between Baseline property distributions and that gained from AGC samples, both irradiated specimens and the unirradiated sister specimens, it is clear that a more in-depth mechanistic understanding of the resulting AGC distributions can be gained through an accurate comparison of the three-point modified flexure test and the standard four-point test. To this end, a modification to the Baseline Graphite Characterization program is planned that will test a large fraction of Baseline specimens under the modified three-point conditions. By greatly increasing this sample population, a more direct comparison can be made between the specimen distributions for the different conditions based on the specific test limitations. At present, it can be seen that a comparison of the four-point Baseline data and the sister specimen data is not complete enough to fully define the test limitations and related results. Until a better understanding of this limitation is gained, the mechanisms behind the ultimate shift in property distributions cannot be confidently made. This limitation will be rectified as the Baseline work continued through sample populations of full-sized billets being slated for the AGC-based three-point test. This addition will greatly enhance the ability to use the data available to both understand the appropriate mechanical behavior and to eventually build modeling and simulation capabilities that can accurately predict the mechanical response of graphite.

The continued evaluations of the candidate nuclear graphite grades will expand to include a number of additional datasets in order to provide the most detailed information on graphite properties. Not only will the mechanical properties testing of the remaining AGC experiments provide information on the effects of temperature and dose on graphite mechanical properties, but will also provide information on additional candidate grades, such as 2114.

From an overall evaluation standpoint, the comparison of AGC-based pre- and post-irradiation data will continue to be evaluated alongside the comprehensive data from the Baseline Graphite Characterization datasets. This comparison and integration of the comprehensive variability ascertained from the baseline data will include not only the mechanical strength data, in a similar manner as was discussed in the report for the AGC-2 data, but will also include the numerous physical property measurements that are being recorded both for AGC and for baseline specimens.

From this data, a true predictive capability for the probabilistic distributions for both physical and mechanical properties will be available in order to develop whole-core analytical tools that will be instrumental in facilitating the design, operation, and life prediction calculations for a VHTR graphite core.

5. REFERENCE

1. PLN-3267, “AGC-2 Characterization Plan.”
2. PLN-3467, “Baseline Graphite Characterization Plan: Electromechanical Testing.”
3. ASTM Standard C749-08, “Standard Test Method for Tensile Stress-Strain of Carbon and Graphite” ASTM International, West Conshohocken, PA (2010).
4. ASTM Standard C651-11, “Standard Test Method for Flexural Strength of Manufactured Carbon and Graphite Articles Using Four-Point Loading at Room Temperature” ASTM International, West Conshohocken, PA (2011).
5. ASTM Standard C695-91, “Standard Test Method for Compressive Strength of Carbon and Graphite” ASTM International, West Conshohocken, PA (2010).
6. ASTM Standard C781-08, “Standard Practice for Testing Graphite and Boronated Graphite Materials for High-Temperature Gas-Cooled Nuclear Reactor Components” ASTM International, West Conshohocken, PA (2014).
7. ORNL/TM-2009/025: Burchell et al. “AGC-1 Sister. Specimen Testing Data Report” May 2009.
8. ASTM Standard D7972-14, “Standard Test Method for Flexural Strength of Manufactured Carbon and Graphite Articles Using Three-Point Loading at Room Temperature,” ASTM International, West Conshohocken, PA (2010).
9. “Errors Associated with Flexure Testing of Brittle Materials,” F. I. Baratta, W. T. Matthews, and G. D. Quinn, U.S. Army Laboratory Command, U.S. Army Materials Technology Laboratory, Watertown, MA, July 1987.
10. “Commencement of Mechanical Testing on Irradiated Advanced Graphite Creep Specimens,” M. C. Carroll, Interoffice Memorandum, Uniform File Code: 8406, August 20, 2014.
11. ASTM Standard D7846.
12. INL/EXT-14 33120, “Initial Comparison of Baseline Physical and Mechanical Properties for the VHTR Candidate Graphite Grades,” Idaho National Laboratory, September 2014.
13. ECAR-2291, “As-Run Physics Analysis for the AGC-2 Experiment Irradiated in the ATR,” Idaho National Laboratory, March 6, 2014.
14. ECAR-2322, “As-Run Thermal Analysis of the AGC-2 Experiment,” Idaho National Laboratory, April 7, 2014.